Optimal Use of LNG Cold Energy in Air Separation Units

*Donghoi Kim, Roxane E. H. Giametta, and Truls Gundersen**

Department of Energy and Process Engineering, Norwegian University of Science and Technology (NTNU), Kolbjørn Hejes vei 1B, NO-7491, Trondheim, Norway

Abstract

One of the solutions to utilizing LNG cold energy at import terminals is supplying it to an ASU, replacing an external refrigeration process and reducing the power consumption. Thus, two different options for the integration of a novel single column ASU process with LNG vaporization have been developed to achieve optimal use of the cold energy. After optimizing the heat integration part, both energy and exergy analyses have been performed to evaluate and compare the two integration options. The results indicate that the single column ASU process, pre-cooled by an LNG stream has a lower specific power consumption (0.281 kWh/kg) than the integration option with a liquid nitrogen production cycle (0.310 kWh/kg). The integration option with pre-cooling also delivers a higher exergy efficiency for different LNG pumping pressure levels, compared to the alternative with a liquid nitrogen production cycle.

1. Introduction

To bring natural gas into distribution networks, transport in liquefied form can be the most economical and convenient solution for remote places. Thus, natural gas is liquefied and transported at -162 °C and slightly above atmospheric pressure by liquefied natural gas (LNG) carriers. Most often, the tail end of the distribution networks and the end-users require the LNG to be in gas phase. Such regasification is achieved at LNG import terminals. In the terminals, the transported LNG is unloaded from the carriers at a typical flow rate of 12,000 cubic meters per hour and filled in storage tanks. The stored LNG is then pumped to a vaporization system at a pressure between 80 and 120 bar depending on the gas export requirements[1]. After being pressurized, the LNG is converted to gas phase by heat exchange in vaporizers. There are two main types of vaporizers on the market: open rack vaporizers (ORV), which represent around 70 % of the installations, and submerged combustion vaporizers (SCV), representing a 20 % share[2]. Other options are ambient air vaporizers (AAV), shell and tube exchange vaporizers (STV) and intermediate fluid vaporizers (IFV)[3]. Several vaporizers are required to achieve the total regasification capacity of a typical import terminal. The best combination of vaporizer types depends on site ambient conditions[4].

Due to the increasing demand for LNG, the total world regasification capacity also expanded to 757.1 million tons per annum (MTPA) in 2015 with 108 regasification terminals[5]. Consequently, a significant amount of LNG cold energy has been wasted to seawater or air in typical regasification processes although it could have been utilized in various processes to improve their efficiency. However, there are several aspects to be considered when recovering the LNG cold energy in other systems. First, the duty and temperatures available for heat integration during LNG regasification depend on the gas distribution pressure[6]. Another common constraint is the long

distance between the cold energy (exergy) available at the regasification terminal and the potential users.

To overcome the distance limitation, carbon dioxide can be liquefied at the LNG terminal and transported in pipelines to for example food processing facilities or buildings requiring air conditioning[7]. Nevertheless, the operating temperature of the refrigeration application is limited to -60 °C due to the freezing point of the intermediate working fluid (CO_2). Therefore, this example cannot recover LNG cold energy in the whole temperature range available during regasification, which will result in sub-optimal use of LNG cold energy.

Low-temperature power generation is another option to utilize the LNG cold energy. However, power production using Rankine cycles does not go below -90 °C when ethane is used as a working fluid[8]. In the case of Brayton cycles, one could go down to -140 °C using nitrogen as a working fluid, but this has not yet been implemented in real applications.

Freezing or evaporation-condensation desalination are also possible options to be integrated with LNG regasification. However, the use of a glycol-water solution as an intermediate working fluid will limit the operating temperature to -15 °C[9]. By using LNG cold energy, heavy hydrocarbons can be extracted from the stored LNG having a heating value above the distribution requirements. This integration covers temperatures from -160 °C but only to -105 °C[10]. Therefore, this option does not fully replace conventional vaporization processes since there is still a considerable amount of cold energy left to be recovered from the LNG.

Unlike the integration options mentioned above, an air separation unit (ASU) is a system that can fit in the temperature range of LNG vaporization. Due to the low operating temperature of air separation units (from -170 °C to -190 °C), which is closer to the LNG temperature than any other options, supplying parts of the cold duty in an ASU is regarded as a promising alternative for

utilizing the cold energy of LNG. Hence, this integration has already been applied in several LNG import terminals since the 1970s[11].

However, air separation has complex process configurations with a single column, double column, or even triple column distillation, including sophisticated internal heat integration[12-13]. Thus, there have been several suggestions for integration of LNG regasification processes with different ASU designs, showing distinctive characteristics[11,14-16]. Most suggestions integrate LNG regasification with conventional two-column or novel single-column ASU processes. Besides, the structure and performance of the ASU processes combined with LNG regasification vary depending on the way LNG cold energy is utilized. Therefore, these integration solutions were simulated and assessed to understand their strengths and weaknesses in depth under fair conditions.

In this work, ASU processes integrated with LNG regasification are categorized based on the method for utilization of LNG cold energy. A single-column ASU configuration is applied as a reference process to be combined with an LNG stream[17]. A comparison between the two systems is conducted by considering both energy and exergy as performance measures. A discussion is also made on the optimal use of LNG cold energy, depending on the integration method.

2. Process design

2.1 Single column ASU

ASU processes differ mainly by the number of distillation columns in the cold box and the operating pressure levels. These differences affect the products (purity, phase and pressure) as well as the power consumption and the capital cost of the ASU. Nitrogen (78.12 mol % and normal boiling point (NBP) of -195.9 °C) and oxygen (20.95 mol % and NBP of -182.9 °C) are the two components normally recovered from the air through the ASU. Noble gases present in the

atmosphere can also be extracted by multi-column processes and further purification of the product streams.

In this work, a single-column ASU process using a recuperative vapor recompression heat pump[17] is selected as a design basis to be integrated with LNG regasification. This novel configuration produces pure nitrogen and intermediate purity oxygen (95 mol %) at atmospheric pressure, which matches the requirements for oxy-combustion applications in coal-based power plants. The advantages of this process, compared to traditional double column ASU processes, are the reduced number of columns and the reduced power consumption (less air compression).

An adjusted version of the novel single column ASU[17] was modeled in HYSYS V9.0[18] and is shown in Figure 1. Mainly, this model is based on the configuration referred to as Cycle 6, which is more practical with respect to deployment. In this process, the air feed (A01) is slightly compressed (i.e. using a fan) to compensate for pressure losses through the system, and then split into streams A04a and A05a. Stream A04a is pressurized and delivered to the main heat exchanger (MHE) to be cooled before being sent to an expander (E-A). This depressurization of cold stream A04f will reduce the cold duty of the MHE, and stream A04g is further cooled in the MHE to be

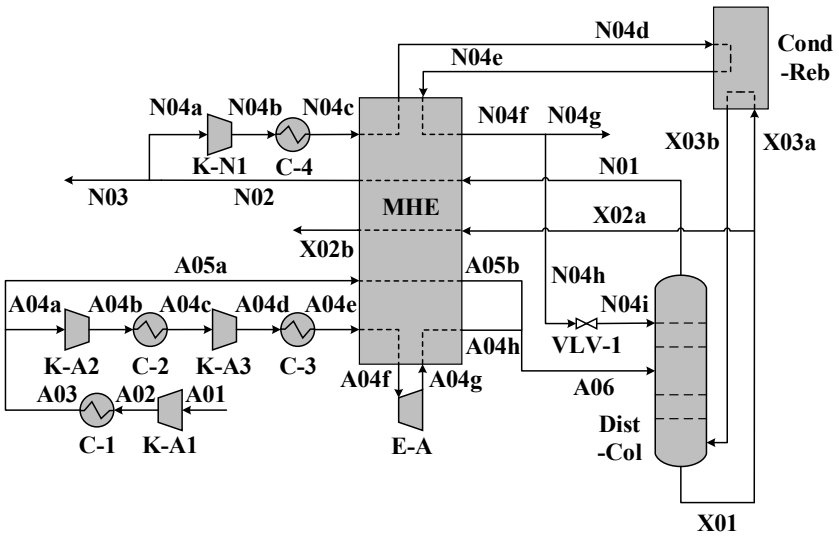

Figure 1. Process flow diagram for the single column ASU (modified from Cycle 6 in ref 17).

slightly condensed. Stream A05a is also cooled in the MHE and mixed with the partially liquefied air stream A04h. The mixed stream A06 is supplied to the distillation column (Dist-Col) at an intermediate level to be separated into a bottom liquid X01 and an overhead vapor N01. The pure nitrogen gas stream (N01) is returned to the MHE to supply refrigeration duty and being warmed to ambient temperature, producing a nitrogen vent stream N03.

A part of the nitrogen product (N04a) is compressed and cooled to a cryogenic temperature in the MHE. The pre-cooled nitrogen stream N04d enters the MHE again via the integrated heat exchanger (Cond-Reb), boiling the liquid oxygen (LO2) product (X01). Then the nitrogen stream that is sub-cooled through the MHE (N04f) is split to provide a liquid nitrogen (LN2) product (N04g) and reflux to the column (N04h) after throttling (N04i). The liquid oxygen stream X01 from the bottom of the column is split into two branches. One branch (X03a) is vaporized in the heat exchanger Cond-Reb, and the other branch (X02a) is sent to the MHE to provide cooling duty and be vaporized to the final oxygen product.

2.2 Single column ASU with an LN2 production cycle (Option 1)

The novel single column ASU process produces very little liquid nitrogen and oxygen since it was primarily aimed at oxy-combustion coal-based power generation. Thus, one of the options to utilize LNG cold energy is to supply additional refrigeration to the ASU to enable it to deliver liquid products, which can be transported long-distance. One way to achieve this integration is connecting a sub-process for liquid nitrogen production to ASU systems[14,16]. Thus, the single column ASU process was modified to include the LN2 production cycle having the LNG stream as a refrigeration source (Figure 2). This integration is referred to as Option 1 in this paper.

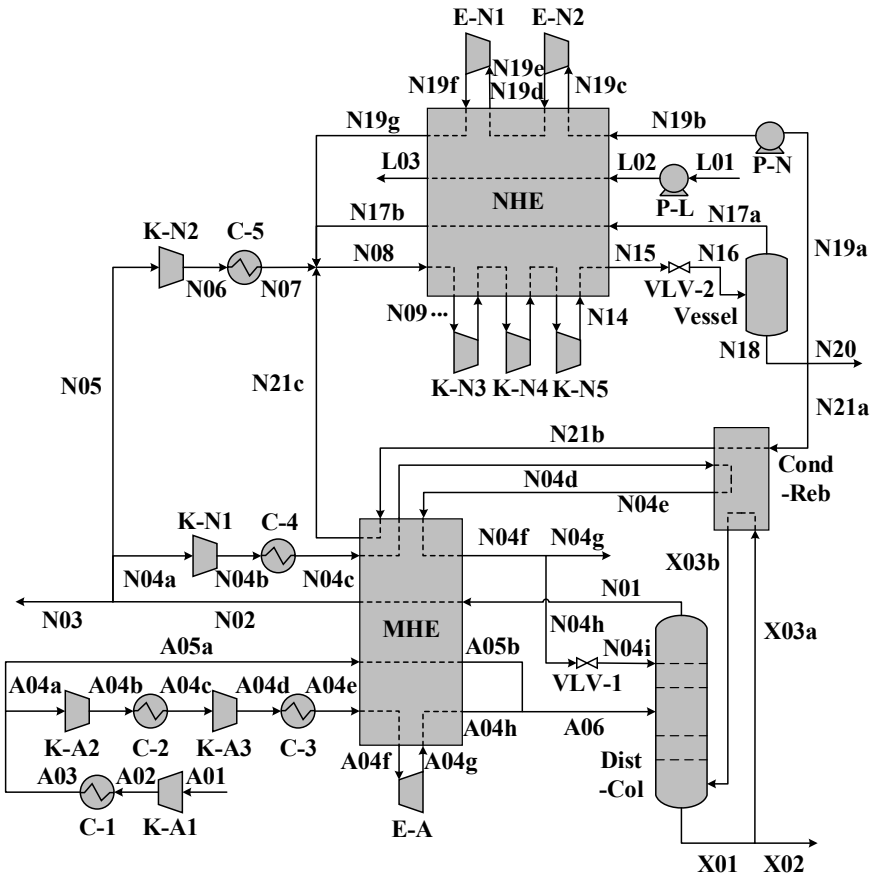

Figure 2. Process flow diagram for the single column ASU with an LN2 production cycle.

This integration scheme has an almost identical structure as the single column ASU except that a part of the nitrogen vent stream (N05) is sent to a liquid nitrogen production system. This recycled nitrogen stream goes through multi-stage compression and intercooling via the nitrogen heat exchanger (NHE), while gasifying the compressed LNG stream L02. The fully condensed nitrogen stream (N15) leaves the NHE and enters a throttling valve to be depressurized before feeding a vessel. The gas stream from the phase separator (N17a) provides a cold duty to the NHE and goes back to the second recycled nitrogen compressor while the liquid stream (N18) is divided into three parts. One (N21a) is used for the cooling demand of the nitrogen reflux (N04d) in the Cond-Reb and the MHE. The second part (N19a) is compressed by a pump (P-N) with a relatively small power consumption and evaporated via the NHE before being depressurized in turbo-

expanders. The expansion will produce power and supply cold duty to the NHE in order to liquefy the recycled nitrogen stream N08. The last part (N20) is then provided as a liquid nitrogen product.

Finally, it should be emphasized that, unlike the single column ASU process, a part of the liquid oxygen product from the ASU (X01) does not need to be supplied to the MHE, rather it is directly extracted as a liquid product (X02).

2.3 Single column ASU with pre-cooling (Option 2)

In Option 1, LNG cold energy is supplied to the NHE where the recycled nitrogen stream is cooled. However, the LNG stream does not exactly match the cold duty of the NHE, increasing the temperature difference in the heat exchanger. Instead, the LNG stream can be used for pre-cooling of air, reflux nitrogen, and the recycled nitrogen stream[15]. By adjusting the pre-cooling temperature, LNG cold energy can be well fit to the cold duty of the pre-cooling heat exchanger, reducing driving forces. The single column ASU with the pre-cooling scheme is referred to as Option 2 in this paper.

For the pre-cooling of air, reflux nitrogen, and recycled nitrogen, the LN2 production system in Option 1 is integrated into the main heat exchanger (MHE) and LNG cold energy is supplied to the MHE. Besides, the cold part of the MHE is separated as an independent heat exchanger (Sub-HE) to sub-cool the air, the reflux nitrogen and the recycled nitrogen as seen in Figure 3.

By splitting the MHE, the intermediate temperature of the air, reflux nitrogen, and the recycled nitrogen stream can be manipulated depending on the state of the LNG stream, resulting in a better temperature match between the streams in the MHE and thus an improved use of the cold LNG. Thus, the LNG stream pumped from a storage tank (L02) provides refrigeration only to the MHE. The typical intermediate temperature will be close to the supplied LNG temperature.

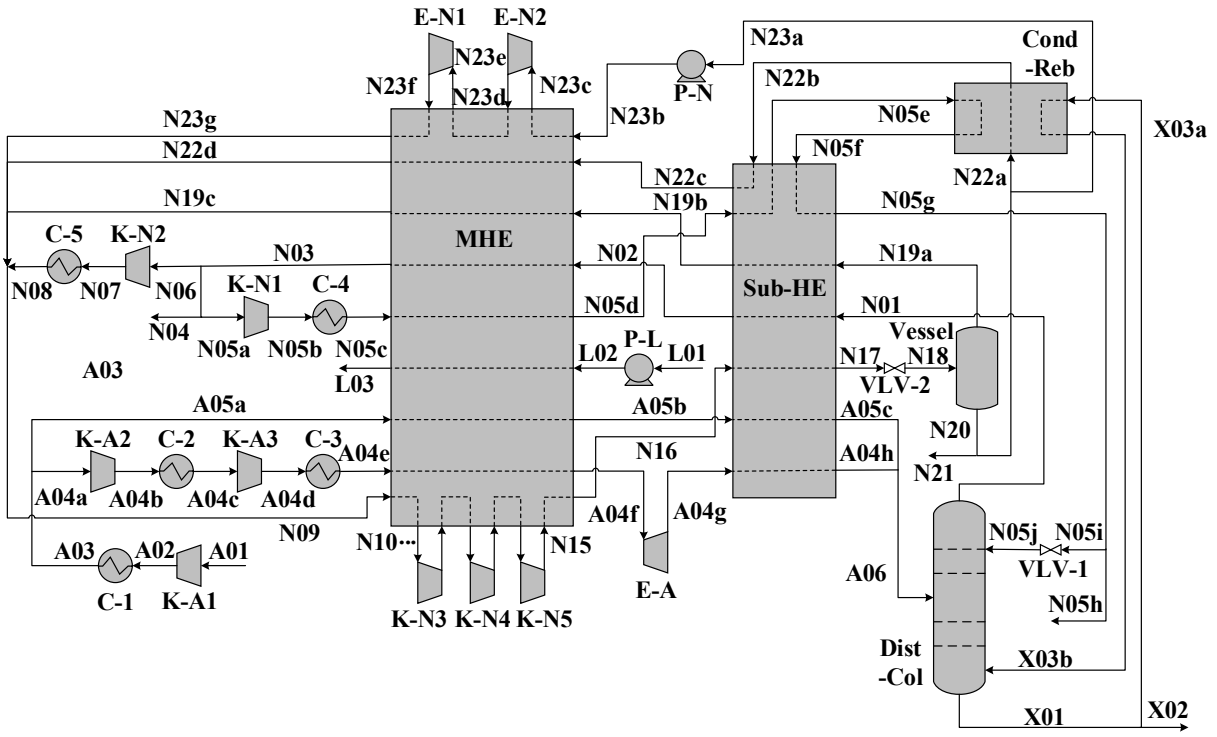

Figure 3. Process flow diagram for the single column ASU with pre-cooling.

3. Simulation conditions and design parameters

3.1 Scope of the models

Cryogenic air separation is performed after air compression and purification where water and other impurities are removed by adsorption on molecular sieves. Then, the purified air is cooled to the dew point temperature and separated by cryogenic distillation in a cold box, which is heavily insulated to limit heat losses[19]. Since the air purification step is not of primary concern in this work, it is disregarded in all the models of ASU processes integrated with LNG vaporization. However, the LNG pumping system is included in the integration schemes. In the case of the reference single column ASU system, a simplified LNG vaporization system was included to evaluate the total performance of the ASU and the regasification process stand-alone so that it can be compared with

the two integration options. The LNG vaporization system is composed of a pump to pressurize the LNG feed and a heater to evaporate the compressed LNG. The stand-alone reference ASU system, which does not include the LNG regasification was also simulated to measure the original performance of the ASU.

Other design specifications for thermodynamic properties and equipment in the processes are indicated in Table S1 in the Supporting Information.

3.2 LNG feed

The required natural gas pressure at the outlet of the LNG regasification terminal depends on the end-users, ranging from 6 to 25 bar for power stations, 30 bar for local distribution and over 60 bar for long-distance distribution[8]. This parameter has a noticeable influence on the performance of the integration solutions because the compression to the selected distribution pressure consumes pumping power and the pressure level affects the available cold energy of the LNG[6]. This work will focus on long-distance gas distribution, selecting a gas outlet pressure of 60 bar for the models. Due to the importance of the LNG pumping pressure, it was varied from 20 bar to 100 bar in order to measure the effect on the process performance in Section 6.2. In the review of existing ASU systems integrated with LNG regasification, the flow rates of the LNG feed range from 8 tons per hour for small-scale to 68 tons per hour for large-scale integration processes, and the larger scale has been the latest trend[11]. Thus, a flow rate of 3300 kmol per hour (equivalent to around 58 tons per hour) was selected for large-scale ASU systems integrated with LNG vaporization. Other design conditions related to LNG are shown in Table S2 in the Supporting Information.

3.3 Air feed

For simplification, the air feed is assumed to consist of nitrogen and oxygen only. Since noble gas production is not studied in this work, the presence of argon, helium, etc. is neglected. Further, it is assumed that the air pre-treatment (not included in the simulation models) completely removes water and carbon dioxide. Conditions of the air feed are provided in Table S3 in the Supporting Information.

3.4 Product specifications

The classic indicator to evaluate ASU designs is the power consumption per amount of liquid nitrogen or oxygen produced. However, the compression work required is varying depending on the quantity of liquid products from the ASU systems. The desired product purities are other factors influencing the performance of the ASU schemes. Thus, the product flow rates and purities were set to be equal for all the ASU processes integrated with LNG regasification.

During the simulation work, the maximum flow rate that could be reached for liquid nitrogen produced from the recycled nitrogen was around 415 kmol per hour with a purity of 99.5 mol % in the single column ASU with an LN2 production cycle. These values were used as specifications for the alternative integration option (ASU with pre-cooling).

Pure liquid oxygen is also produced in all the models. The flow rate of liquid oxygen is varying based on the configuration of the integration systems since it is constrained by the reflux needed in the distillation column and the heat balance of the integrated condenser-reboiler. Thus, the amount of liquid oxygen product was fixed at the quantity of the vapor oxygen produced in the reference single ASU system, which is one of the design targets for the integration schemes. None of the processes provided gaseous oxygen, however, they do produce a gaseous nitrogen stream, which is vented to the atmosphere.

The reference single column ASU was manipulated to produce liquid nitrogen from the nitrogen reflux in order to be compared with the integration schemes delivering liquid products. Due to the lack of cold duty without LNG cold energy utilization, the maximum achievable amount of liquid nitrogen was 158 kmol per hour based on the one-column ASU. Thus, this value is set for the liquid nitrogen product from the nitrogen reflux in the stand-alone single column ASU and the two integration options. However, sufficient amounts of pure gaseous oxygen and nitrogen with a purity above 99.5 mol % are produced in the stand-alone single column ASU.

Apart from product flow rate and purity, other conditions such as temperature and pressure will vary among the ASU processes, thus having different exergy values. Besides, there will always be a minor difference between the specifications and the actual products. Thus, evaluation and comparison based on energy may not be adequate. Exergy efficiency, however, can account for varying compositions, flow rates, temperatures and pressures of the product streams, as will be explained in Section 5. Thus, the temperature and pressure levels of the products will vary depending on the ASU processes, accepting a marginal difference in their purity and flow rate.

The LNG stream supplying a cold duty to existing ASU systems integrated with LNG regasification is generally warmed to ambient temperature either in cryogenic heat exchangers or intercoolers for air and nitrogen compressors[11,15-16]. This leads to large temperature gaps in the cryogenic exchangers and the intercoolers, causing significant amounts of entropy generation. Thus, the outlet temperature of the LNG product was not restricted to ambient temperature in order to find optimal use of the LNG cold energy in the integration schemes. The detailed specifications for ASU products are summarized in Table 1.

Table 1. Product specifications for the ASU systems.

Condition	Unit	LN2*	LN2**	LO2	LNG
Temperature	°C	vary	vary	vary	vary
Pressure	bar	4.5	vary	vary	60
Purity	mol %	> 99.5	> 99.5	> 99.9	-
Flow rate	kmol/h	158	415	499	3300

*LN2 extracted from the nitrogen reflux
**LN2 extracted from the recycled nitrogen

4. Optimization

To perform a fair comparison between the two integration options, they were both subject to some kind of optimization. Since optimizing a distillation column is complex, the design conditions related to the column were disregarded. The variables related to the air compressors, and the high pressure as well as the molar flow rate of the nitrogen reflux were not adjusted, in order to conform with the reference ASU design. This will allow focusing on the heat integration part of the ASU systems, indicating the actual potential of utilizing the LNG cold energy. Thus, all the inlet temperatures and outlet pressures of the multi-stage compressors for the recycled nitrogen were set as variables. The final temperature of the recycled nitrogen to be throttled before producing liquid nitrogen is also considered a variable. In addition, all the inlet temperatures and outlet pressures of the multi-stage expanders for the recycled nitrogen were also defined as variables in addition to the pressure level of the booster pump for the recycled nitrogen. Besides, the molar flow rate of the by-passed air, the recycled nitrogen and the liquefied nitrogen sent to the integrated heat exchanger (Cond-Reb) were selected as variables. For integration Option 2, the intermediate temperatures of the streams flowing between the MHE and the Sub-HE were set as extra variables. The values of the ranges for the variables are listed in Table S4 for Option 1 and Table S5 for Option 2 in the Supporting Information. With the decision variables $\mathbf{x}$, the two

integration schemes were optimized for the objective function and constraints in Eq (1), where $a \in H$ and $b \in K$.

$$\begin{aligned} \min_{\mathbf{x}} \quad & f(\mathbf{x}) = \frac{\dot{W}_{\text{net}}}{\dot{m}_{\text{LN2}} + \dot{m}_{\text{LO2}}} \\ \text{subject to} \quad & \Delta T_{\text{min,a}} \geq 1 \\ & Pr_{\text{b}} \leq 3 \\ & \mathbf{x}_{LB} \leq \mathbf{x} \leq \mathbf{x}_{UB} \end{aligned} \tag{1}$$

H represents the set of cryogenic heat exchangers and K is the set of compressors. The objective is to minimize power consumption per amount of total liquid products. A minimum temperature difference of 1 K is applied for all heat exchangers as a constraint, which is a common practice in cryogenic processes[20]. The maximum pressure ratio of compressors is set to 3. The optimization is performed by sequential quadratic programming (SQP) due to the nonlinearity of the system. The optimization results are shown in Table S4 and Table S5 in the Supporting Information for Option 1 and Option 2 respectively.

5. Exergy analysis

Exergy is the maximum available work obtained by bringing a system to equilibrium with its environment. Thus, exergy analysis, which is a combination of the first and second laws of thermodynamics, is based not only on the condition of a system but also the environment. Different energy sources having different qualities such as temperature, pressure and composition can be measured by exergy. These features make exergy efficiency more reliable than energy efficiency, showing the real performance of processes. Exergy analysis also allows identifying where exergy is destroyed in a process, in other words, the location of entropy generation. This gives guidelines

to improve efficiency by highlighting units having the largest exergy destruction. Thus, in this work, exergy analysis is regarded as a valuable post design tool together with specific power consumption.

Exergy analysis requires decomposition of exergy, which can vary depending on the type of process. Thus, various exergy decompositions have been suggested, showing different definitions of exergy efficiency[21-25]. In this work, one of the approaches to exergy decomposition was used to perform an objective and consistent exergy analysis[25]. Kinetic, potential, electrical and nuclear exergies were not considered in the exergy decomposition. Thus, the total exergy of a material stream is given by:

$$\dot{E}^{\mathrm{Total}} = \dot{E}^{\mathrm{TM}} + \dot{E}^{\mathrm{Ch}} \tag{2}$$

where $\dot{E}^{\mathrm{TM}}$ and $\dot{E}^{\mathrm{Ch}}$ denote thermo-mechanical and chemical exergies respectively. Thermo-mechanical exergy is commonly decomposed into pressure based ($\dot{E}^{\mathrm{p}}$) and temperature based exergy ($\dot{E}^{\mathrm{T}}$) as seen in Eqs. (3)-(5). The temperature-based part is defined by bringing the system from its initial temperature T to the environment temperature T_0 at constant initial pressure p while the pressure-based part is bringing the system from p to p_0 at constant temperature T_0.

$$\dot{E}^{\mathrm{TM}} = \dot{E}^{\mathrm{T}} + \dot{E}^{\mathrm{p}} \tag{3}$$

$$\dot{E}^{\mathrm{T}} = \dot{H}(T,p) - \dot{H}(T_0,p) - T_0[\dot{S}(T,p) - \dot{S}(T_0,p)] \tag{4}$$

$$\dot{E}^{\mathrm{p}} = \dot{H}(T_0,p) - \dot{H}(T_0,p_0) - T_0[\dot{S}(T_0,p) - \dot{S}(T_0,p_0)] \tag{5}$$

The chemical exergy of a system refers to the deviation in its chemical composition from reference substances present in the environment. Chemical exergy of a material stream can also be decomposed:

$$\dot{E}^{\mathrm{Ch}} = \dot{E}^{\mathrm{Conc}} + \dot{E}^{\mathrm{Reac}} \quad (6)$$

where $\dot{E}^{\mathrm{Conc}}$ and $\dot{E}^{\mathrm{Reac}}$ are the concentrational and reactional exergies respectively. These exergy components are defined by:

$$\dot{E}^{\mathrm{Conc}} = \dot{H}(T_0, p_0) - \sum_i \dot{H}_i^{\mathrm{pure}}(T_0, p_0) - T_0\left[\dot{S}(T_0, p_0) - \sum_i \dot{S}_i^{\mathrm{pure}}(T_0, p_0)\right] \quad (7)$$

$$\dot{E}^{\mathrm{Reac}} = \Sigma \dot{n}_i \bar{e}_{i,0}^{\mathrm{Chem}} \quad (8)$$

Concentrational exergy represents the reduction in chemical exergy due to mixing. Reactional exergy is the sum of the standard chemical exergy values of each pure component in a mixture ($\bar{e}_{i,0}^{\mathrm{Chem}}$). The standard chemical exergy values were calculated by implementing the existing reference conditions of the environment[22].

This work applies the Exergy Transfer Effectiveness (*ETE*) to evaluate the exergy efficiency of the ASU systems integrated with LNG regasification[26]. This exergy efficiency was developed for low-temperature processes, offering a general mathematical expression. Still, the use of the *ETE* is limited to changes in temperature and pressure of a system (i.e. only thermo-mechanical exergy). Thus, an extended version of ETE recently developed in our group has been used to analyze the integration schemes by including the concentrational and reactional exergy terms. Consequently, the extended definition can handle all changes in flow rate, concentration, pressure, and temperature in the ASU systems integrated with LNG regasification. Besides, this indicator can evaluate and compare the performance of the integration processes, even in cases with different products, due to the definition of the extended *ETE*.

ETE is defined as the ratio between exergy sinks and exergy sources as shown by Eq. (9).

$$ETE = \frac{\sum \text{Exergy Sinks}}{\sum \text{Exergy Sources}} \tag{9}$$

An exergy increase of a process or unit is considered as an exergy sink, while an exergy decrease indicates an exergy source. Likewise, compression work is an exergy source, while expansion work is an exergy sink.

The extended *ETE* with the four exergy components ($\dot{E}^{\mathrm{T}}, \dot{E}^{\mathrm{p}}, \dot{E}^{\mathrm{Conc}}, \dot{E}^{\mathrm{Reac}}$) can then be defined by Eqs. (10)-(12), where $j \in C, k \in I, m \in O$.

$$ETE = \frac{\sum_j \left(\Delta \dot{E}^j\right)^+ + \dot{W}_{\mathrm{Exp}}}{\sum_j \left(\Delta \dot{E}^j\right)^- + \dot{W}_{\mathrm{Comp}}} \tag{10}$$

where

$$\left(\Delta \dot{E}^j\right)^+ = \begin{Bmatrix} \sum_m \dot{E}_m^j - \sum_k \dot{E}_k^j & if \sum_k \dot{E}_k^j < \sum_m \dot{E}_m^j \\ 0 & if \sum_k \dot{E}_k^j > \sum_m \dot{E}_m^j \end{Bmatrix} \tag{11}$$

$$\left(\Delta \dot{E}^j\right)^- = \begin{Bmatrix} 0 & if \sum_k \dot{E}_k^j < \sum_m \dot{E}_m^j \\ \sum_k \dot{E}_k^j - \sum_m \dot{E}_m^j & if \sum_k \dot{E}_k^j > \sum_m \dot{E}_m^j \end{Bmatrix} \tag{12}$$

Eqs. (10)-(12) represent the *ETE* where C is the set of four exergy components, I is the set of inlet streams, and O is the set of outlet streams.

6. Results and discussion

6.1 Comparison of alternatives

In this section, the simulation results of the two different ASU systems integrated with LNG vaporization are assessed and compared with the reference single column ASU process. Specific power consumption per unit mass of liquid products is measured as a process performance index, and Table 2 indicates that integration Option 2 has smaller specific power consumption than Option 1 with almost the same amount of liquid products. The specific power for the reference ASU system was significantly larger since the process was originally developed for gas products. Thus, the *ETE* that can handle differences in products was calculated for all the ASU processes. The exergy efficiency values show that integration Option 2 is again the most efficient process followed by Option 1 and the reference ASU system.

Table 2. Simulation results for the reference single column ASU and its integration schemes with LNG regasification.

	Recycled N_2 [kmol/h]	LN2 [kg/h]	LO2 [kg/h]	Power consumption [kWh/kg]	Exergy destruction [kW]	*ETE* [%]
ASU	3639	4429	-	1.346	9979	47.93
Option 1	3730	16067	15975	0.310	7337	57.34
Option 2	3749	16076	15975	0.281	6158	61.05

The results in Table 2 clearly indicate that integration of an ASU with LNG regasification reduces power consumption and improves exergy efficiency for the entire system. The entries in Table 2 for ASU (1st row) is for stand-alone ASU and LNG regasification (i.e. not integrated). Both Option 1 and Option 2 show that the total system efficiency is significantly improved compared to the reference single column ASU, since considerably less LNG cold exergy is wasted in the regasification process. Nevertheless, the two integration options will have a lower exergy efficiency than the ideal case where the stand-alone ASU is assumed to receive the maximum work

that can be produced from the cold energy utilized in integration Option 1 and 2. In that case, the *ETE* of the stand-alone ASU reaches 79.25 % and 78.93 % respectively.

Option 2 required the largest flow rate of recycled nitrogen, followed by Option 1 and the reference ASU system as seen in Table 2. Table 3 shows that Option 2 also demands the largest heat exchange area (*UA*) among the three cases due to lower values for log mean temperature difference (*LMTD*). This will result in a higher capital cost for Option 2 than the other alternatives. However, the low *LMTD* values indicate a close to optimal temperature match in the heat exchangers with the cold LNG stream, thus improving the process efficiency. In the case of Option 1, an optimal heat integration in the MHE and the NHE was not possible, resulting in large *LMTD*s. This also explains the higher exergy efficiency of Option 2 than Option 1.

Table 3. Heat exchangers in the reference single column ASU process and its integration schemes with LNG regasification.

		ASU		Option 1			Option 2		
	Unit	MHE	Cond -Reb	MHE	NHE	Cond -Reb	MHE	Sub -HE	Cond -Reb
ΔT_{min}	[K]	1.00	1.00	1.00	1.00	1.00	1.00	1.00	1.00
LMTD	[K]	3.10	1.13	7.82	2.42	1.26	2.09	3.87	1.26
UA	[MW/K]	2.62	1.25	0.91	5.83	1.90	8.77	0.22	1.90

6.2 Sensitivity analysis

The pressure level of the LNG product is usually dependent on the conditions of gas distribution networks. Thus, the pumping pressure of the stored LNG was varied from 20 bar to 100 bar in order to measure the effect of the different properties of LNG cold energy on the two integration schemes. The two integration options were also optimized under the different LNG pressure levels to find optimal operating conditions. The results illustrated in Figure 4 indicate that the specific

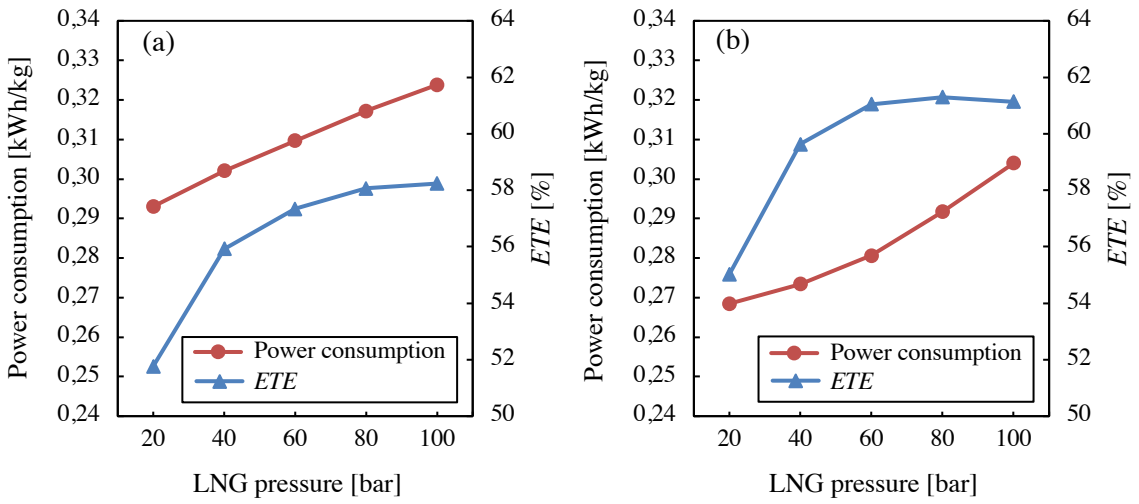

Figure 4. Variation of specific power consumption and exergy efficiency in integration Option 1 (a) and Option 2 (b) for different values of LNG pressure.

power consumption increases with LNG pressure for both Option 1 and Option 2. The power consumption was increased by 10.6 % in Option 1 and 13.4 % in Option 2 when the pressure level was increased from 20 bar to 100 bar. This shows that Option 2 has a larger penalty for achieving an optimal heat integration with increased pressure than Option 1.

Regarding exergy efficiency, the *ETE* value for Option 1 increases with the LNG pressure, showing only a marginal increase after 80 bar as illustrated in Figure 4. The exergy efficiency for Option 2 even experiences a small decrease at 100 bar, explaining the sharper increase in specific power consumption with the LNG pressure than Option 1. Nevertheless, integration Option 2 has a smaller specific power consumption and a higher exergy efficiency at any given LNG pressure levels.

When it comes to exergy destruction, Figure 5 demonstrates that the main sources of thermodynamic losses for both Option 1 and Option 2 are turbo-machinery, followed by heat exchangers and valves, while mixers represents small losses. The amount of exergy destruction in

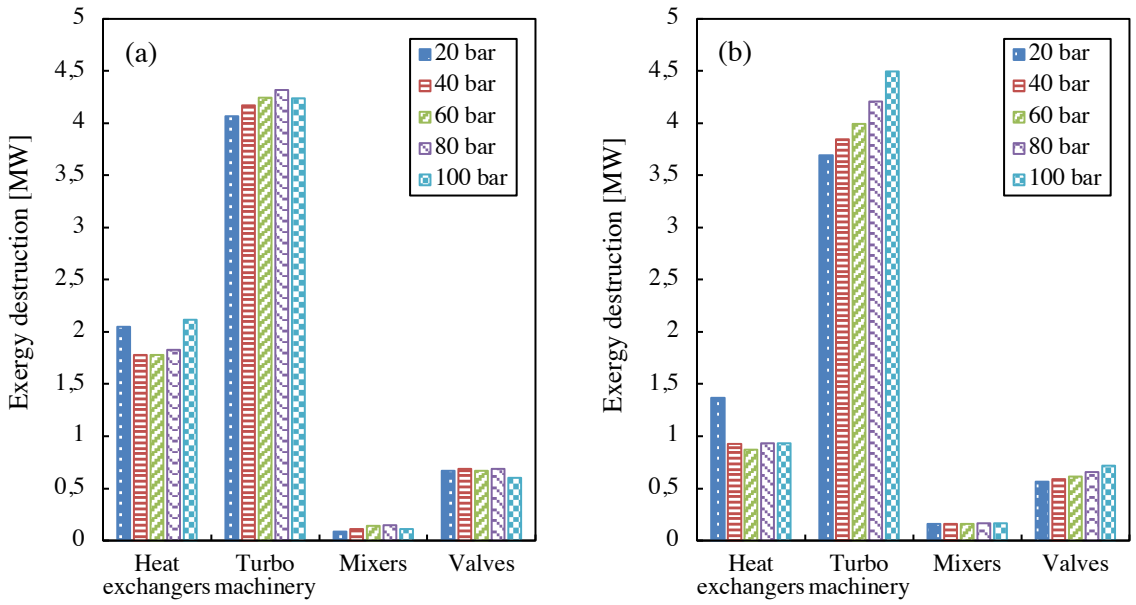

Figure 5. Variation of exergy destruction for main equipment in integration Option 1 (a) and Option 2 (b) for different values of LNG pressure.

Option 2 is smaller than Option 1, especially in the sum of turbo-machinery and heat exchangers, thus resulting in an efficient work and heat exchange network with the cold LNG stream. The changes in exergy destruction for heat exchangers as function of LNG pressure is similar for Option 1 and Option 2. The amount of destruction decreases up to 60 bar and then increases for higher pressures, indicating that the optimal temperature match in the heat exchangers will be achieved at the LNG pressure of 60 bar. This trend in the exergy destruction with LNG pressure explains the considerable improvement of the *ETE* until 60 bar in Figure 4. Besides, the increase in exergy destruction after 60 bar is one of the reasons for the marginal increase in the exergy efficiency over 60 bar.

Unlike heat exchangers, the exergy destruction in turbo-machinery was proportional to the LNG pressure level for both integration options. The main contributor to this increment is the LNG pump, having a larger loss with a higher outlet pressure. However, for Option 1 at 100 bar, the

exergy destruction in the turbo-machinery was slightly reduced. This decrease is a consequence of the inadequate temperature match in the heat exchangers, requiring less pressure ratio in the recycled nitrogen expanders. The poor heat integration also results in smaller pressure drops in some throttling valves, which is the reason for the sudden decrease in exergy destruction for integration Option 1 at 100 bar. Nevertheless, the total exergy destruction of Option 1 at 100 bar is still the largest compared to other LNG pressure levels.

The units that are accounting for the largest share of the exergy destruction in heat exchangers are the NHE in Option 1 and the MHE in Option 2, which are the exchangers integrated with the LNG cold stream. Thus, the temperature difference between hot and cold composite curves in the two heat exchangers is plotted in Figure 6 to investigate their performance for different LNG pressures.

When the LNG pressure is 20 bar, the NHE has a significant temperature difference at around - 80 °C for the hot composite, increasing irreversibilities. This considerable gap contributed to large exergy destructions in heat exchangers as depicted in Figure 5. At the LNG pressure of 100 bar, the NHE also shows a large temperature difference at around -100 °C.

The exergy destruction of the NHE at 100 bar shows a lower temperature difference in the hot end of the exchanger compared to other pressure levels. However, the penalty of the large temperature difference at colder temperatures exceeds the benefit of reduced temperature difference in the hot-end, resulting in the largest exergy destruction for the heat exchangers as seen in Figure 5. This is due to the characteristics of entropy generation caused by the temperature difference in a heat exchanger, which increases exponentially at lower temperatures. Thus, smaller driving forces at lower temperatures in a heat exchanger minimize total irreversibilities, while allowing an optimal use of heat exchanger area[27].

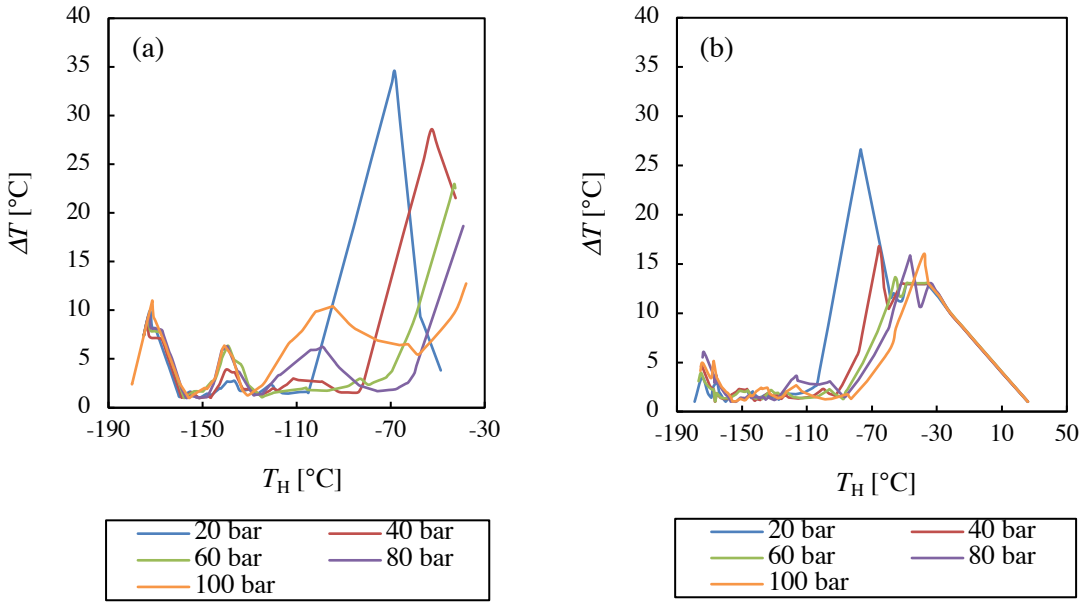

Figure 6. Temperature difference in the NHE for integration Option 1 (a) and in the MHE for integration Option 2 (b) for different values of LNG pressure.

This indicates that the temperature difference profiles at 40 bar and 60 bar are close to the optimal distribution of driving forces, resulting in the lowest exergy destruction, as illustrated in Figure 5. The situation at 80 bar is similar to 100 bar in the sense that larger temperature differences in the middle of the NHE cannot be compensated by smaller temperature differences in the hot end, thus exergy losses are increased compared to the 60 bar case.

Similar to the NHE in Option 1, the temperature difference in the MHE in Option 2 at the LNG pressure of 20 bar is considerably larger at around -80 °C compared to other LNG pressure levels, resulting in the largest exergy destruction in heat exchangers, as seen in Figure 5. At LNG pressures higher than 20 bar, the distributions of the driving forces are almost identical, providing similar exergy destruction values as shown in Figure 5. One noticeable feature is that integration Option 2 managed to keep the temperature difference below 5 K in the cold end of the MHE for all LNG pressure levels. Therefore, the exergy destruction values of heat exchangers in Option 2

at any LNG pressure levels are lower than Option 1. This means that integration Option 2 provides an excellent flexibility to manipulate the system to achieve optimal distribution of the driving forces in the heat exchangers, leading to a higher process efficiency.

Exergy destruction will not be a sufficient explanation to the changes in exergy efficiency with various LNG pressure levels since it is also related to the products of the integration schemes. In this work, the LNG stream leaving the integration processes is the product that has the largest effect on the changes in exergy efficiency, since the conditions of the final LNG product vary depending on the LNG pumping pressure levels. Other products such as LN2 and LO2 do not experience a substantial change in exergy values after optimizing the two integration options with different LNG pressure levels. Figure 7 illustrates the temperature and pressure based exergy values of the final LNG product and the total exergy destruction for the two integration processes. Regarding the LNG product, it is obvious that the pressure based exergy increases with LNG pumping pressure. However, the temperature based exergy decreases with increasing LNG pressure. This is related to the special behavior of temperature based exergy below ambient temperature, i.e. it decreases with higher temperatures, which is opposite of the behavior above ambient.

Thus, the thermo-mechanical exergy of the final LNG will increase less at larger LNG pumping pressures. Such slow increase in exergy of the LNG product is compensated by the larger total exergy destruction with higher LNG pressures as seen in Figure 7. Therefore, the improvement in exergy efficiency starts diminishing after 40 bar where the lowest exergy destruction occurs in both integration options. In the case of Option 2, the exergy efficiency even indicates a decrease after 60 bar due to the sharp increase in total exergy destruction after 40 bar.

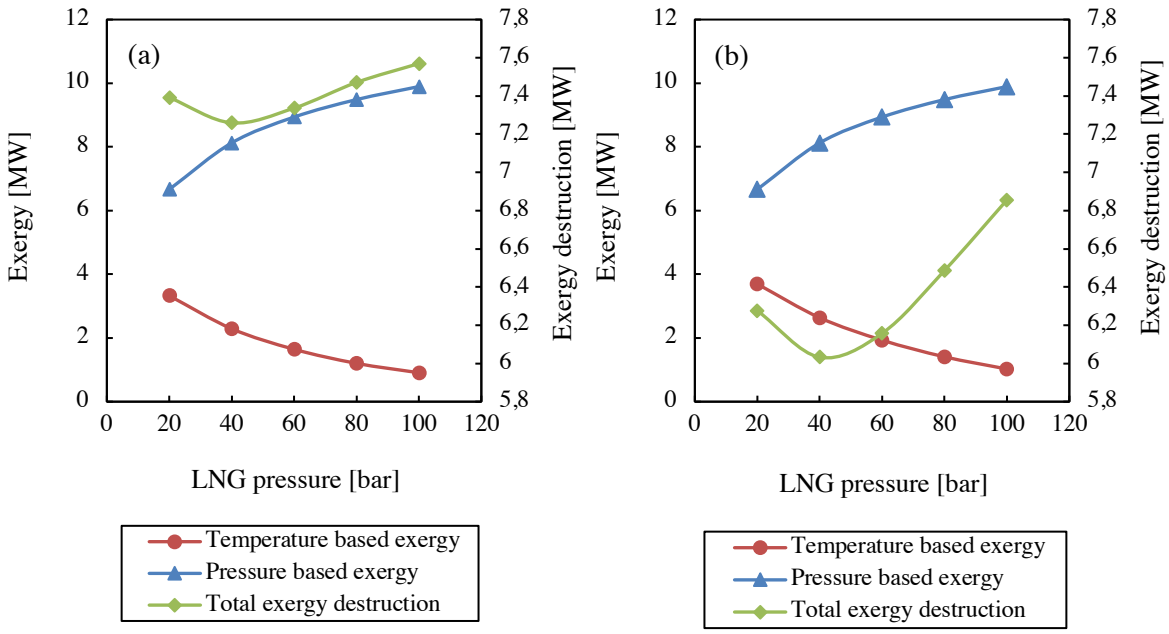

Figure 7. Variation of temperature and pressure based exergy of the LNG product and total exergy destruction in Option 1 (a) and Option 2 (b) for different values of LNG pressure.

7. Discussions and further work

A single column air separation unit (ASU) has been integrated with an LNG stream in two different ways to try to achieve the best possible utilization of the cold energy available from LNG regasification. The cold energy of the LNG stream has been used as an extra refrigeration source either in a liquid nitrogen production cycle (Option 1) or for pre-cooling of air and nitrogen streams (Option 2). After optimization, energy and exergy analyses have been applied to measure the performance of the two different integration schemes.

The energy analysis indicates that the single column ASU process with pre-cooling from LNG regasification has a lower specific power consumption (0.281 kWh/kg) than the integration option with a liquid nitrogen production cycle (0.310 kWh/kg). Integration Option 2 also shows a higher exergy efficiency than Option 1 due to an improved heat integration with the cold LNG stream,

resulting in smaller temperature differences in the heat exchangers. However, Option 2 will require the largest capital cost due to a larger recycled nitrogen flow rate and larger heat exchanger area.

A sensitivity analysis with different LNG pumping pressure levels shows that the specific power consumption is increased with higher LNG pressure for both integration options. This indicates that the improved heat integration (smaller driving forces) resulting in reduced compression power does not compensate for the power consumption required to increase LNG pressure. On the other hand, the exergy efficiency increased with the LNG pumping pressure since the exergy values of the products also increased. This is not considered in energy analysis, which is an inaccurate performance index for such processes. With different LNG pressures, Option 2 consistently has a higher exergy efficiency than Option 1, since this integration scheme is able to keep the driving forces in the heat exchangers low independent of the pressure level. Particularly, Option 1 shows a large temperature difference in the nitrogen heat exchanger at the lowest and highest LNG pressure levels, causing a significant increase in exergy destruction.

Unlike existing integration solutions between ASU processes and LNG regasification, the integration schemes studied in this work result in a final LNG product that still has a low temperature. This could be utilized in other low temperature applications and represents an additional benefit from the solutions proposed in this paper. Hence, a proper selection of an additional process utilizing the cold LNG product should be considered in the case of ASU processes integrated with LNG regasification in order to further improve the utilization of the LNG cold exergy.

Supporting Information

This information is available free of charge via the Internet at http://pubs.acs.org/

Design conditions for the ASU processes and optimization variables with the best solution.

ACKNOWLEDGMENT

The authors would like to acknowledge Statoil for financial support.

AUTHOR INFORMATION

Corresponding Author

Tel.: +47 73593721. E-mail: truls.gundersen@ntnu.no.

NOMENCLATURE

Roman letters

C = set of four exergy components

$\dot{E}$ = exergy rate [kW]

$\bar{e}$ = specific exergy [kJ/kmol]

ETE = exergy transfer effectiveness [%]

H = set of cryogenic heat exchangers

$\dot{H}$ = enthalpy rate [kW]

I = set of inlet streams

K = set of compressors

$LMTD$ = log mean temperature difference [K]

$\dot{m}$ = mass flow rate [kg/s]

$\dot{n}$ = mole flow rate [kmol/s]

O = set of outlet streams

p = pressure [bar]

Pr = pressure ratio [-]

$\dot{S}$ = entropy rate [kW]

T = temperature [K]

UA = heat exchanger conductance [MW/K]

$\dot{W}$ = power [kW]

$\mathbf{x}$ = decision variables

Greek letters

ΔT = temperature difference between hot and cold composite curves [K]

ΔT_{min} = minimum approach temperature [K]

Subscripts and superscripts

0 = ambient conditions

a = cryogenic heat exchanger

b = compressor

Ch = chemical exergy

Comp = compressors

Conc = concentrational exergy

Exp = expanders

H = hot composite curve

i = chemical component

j = exergy component

k = inlet stream

LB = lower bound

LN2 = liquid nitrogen

LO2 = liquid oxygen

m = outlet stream

p = pressure based exergy

Pure = pure component

Reac = reactional exergy

T = temperature based exergy

TM = thermo-mechanical exergy

Total = total exergy of a stream

UB = upper bound

REFERENCES

(1) Wang, M.; Zhang, J.; Xu, Q., A novel conceptual design by integrating NGL recovery and LNG regasification processes for maximum energy savings. *AIChE Journal* **2013,** *59* (12), 4673-4685.

(2) Mokhatab, S.; Mak, J. Y.; Valappil, J. V.; Wood, D. A., In *Handbook of Liquefied Natural Gas*, Gulf Professional Publishing: Boston, 2014.

(3) Egashira, S., LNG Vaporizer for LNG Re-gasification Terminal. *Kobelco Technology Review* **2013,** *32*, 64-69.

(4) Patel, D.; Mak, J.; Rivera, D.; Angtuaco, J., LNG vaporizer selection based on site ambient conditions. In *The 17th International Conference & Exhibition on Liquefied Natural Gas*, Houston, Texas, 2013.

(5) IGU *2016 World LNG Report*; International Gas Union: Fornebu, Norway, 2016.

(6) Kanbur, B. B.; Xiang, L.; Dubey, S.; Choo, F. H.; Duan, F., Cold utilization systems of LNG: A review. *Renewable and Sustainable Energy Reviews* **2017,** *79* (Supplement C), 1171-1188.

(7) La Rocca, V., Cold recovery during regasification of LNG part two: Applications in an Agro Food Industry and a Hypermarket. *Energy* **2011,** *36* (8), 4897-4908.

(8) Romero Gómez, M.; Ferreiro Garcia, R.; Romero Gómez, J.; Carbia Carril, J., Review of thermal cycles exploiting the exergy of liquefied natural gas in the regasification process. *Renewable and Sustainable Energy Reviews* **2014,** *38* (Supplement C), 781-795.

(9) Efrat, T., Utilizing Available "Coldness" From Liquefied Natural Gas (LNG) Regasification Process for Seawater Desalination. In *International Desalination Association World Congress 2011*, IDA: Perth, Australia, 2011.

(10) Uwitonze, H.; Han, S.; Jangryeok, C.; Hwang, K. S., Design process of LNG heavy hydrocarbons fractionation: Low LNG temperature recovery. *Chemical Engineering and Processing: Process Intensification* **2014,** *85* (Supplement C), 187-195.

(11) Xu, W.; Duan, J.; Mao, W., Process study and exergy analysis of a novel air separation process cooled by LNG cold energy. *Journal of Thermal Science* **2014,** *23* (1), 77-84.

(12) van der Ham, L. V.; Kjelstrup, S., Exergy analysis of two cryogenic air separation processes. *Energy* **2010,** *35* (12), 4731-4739.

(13) Kerry, F. G., *Industrial gas handbook: gas separation and purification*. CRC Press: 2007.

(14) Jieyu, Z.; Yanzhong, L.; Guangpeng, L.; Biao, S., Simulation of a Novel Single-column Cryogenic Air Separation Process Using LNG Cold Energy. *Physics Procedia* **2015,** *67*, 116-122.

(15) Mehrpooya, M.; Moftakhari Sharifzadeh, M. M.; Rosen, M. A., Optimum design and exergy analysis of a novel cryogenic air separation process with LNG (liquefied natural gas) cold energy utilization. *Energy* **2015,** *90*, 2047-2069.

(16) Tesch, S.; Morosuk, T.; Tsatsaronis, G., Advanced exergy analysis applied to the process of regasification of LNG (liquefied natural gas) integrated into an air separation process. *Energy* **2016,** *117, Part 2*, 550-561.

(17) Fu, C.; Gundersen, T., Recuperative vapor recompression heat pumps in cryogenic air separation processes. *Energy* **2013,** *59*, 708-718.

(18) Aspen Technology Inc., *Aspen HYSYS V9*, Aspen Technology Inc.: Cambridge, MA, 2016.

(19) Agrawal, R.; Herron, D. M., AIR LIQUEFACTION: DISTILLATION. In *Encyclopedia of Separation Science*, Academic Press: Oxford, 2000; pp 1895-1910.

(20) Higginbotham, P.; White, V.; Fogash, K.; Guvelioglu, G., Oxygen supply for oxyfuel CO2 capture. *International Journal of Greenhouse Gas Control* **2011,** *5* (Supplement 1), S194-S203.

(21) Kotas, T. J., *The exergy method of thermal plant analysis*. Butterworths: London, 1985.

(22) Szargut, J., Chemical exergies of the elements. *Applied Energy* **1989,** *32* (4), 269-286.

(23) Brodyansky, V. M.; Sorin, M. V.; Goff, P. L., *The Efficiency of Industrial Processes: Exergy Analysis and Optimization*. Elsevier: Amsterdam, 1994.

(24) Bejan, A.; Tsatsaronis, G.; Moran, M., *Thermal Design and Optimization*. 1 ed.; John Wiley & Sons, Inc.: New York, 1995.

(25) Marmolejo-Correa, D.; Gundersen, T., A comparison of exergy efficiency definitions with focus on low temperature processes. *Energy* **2012,** *44* (1), 477-489.

(26) Marmolejo-Correa, D.; Gundersen, T., A new efficiency parameter for exergy analysis in low temperature processes. *International Journal of Exergy* **2015,** *17* (2), 135-170.

(27) Austbø, B.; Gundersen, T., Impact of problem formulation on LNG process optimization. *AIChE Journal* **2016,** *62* (10), 3598-3610.

Graphical TOC Entry